Aus dem Institut für Neurophysiologie
der Medizinischen Fakultät Charité – Universitätsmedizin Berlin

DISSERTATION

Dynamics and mechanisms of blood-brain barrier dysfunction, cell damage and altered cerebral perfusion after cortical photothrombosis

zur Erlangung des akademischen Grades
Medical Doctor - Doctor of Philosophy (MD/PhD)

vorgelegt der Medizinischen Fakultät
Charité – Universitätsmedizin Berlin

von

Karl Schoknecht

aus Potsdam-Babelsberg

Datum der Promotion: 26.02.2016

Table of Contents

Abstract

Focal cerebral ischemia is one of the main causes of death and disability worldwide. An ischemic core and a surrounding dysfunctional region that is susceptible to cell injury often characterize the lesion. Assessing the propensity of the peri-ischemic brain to undergo secondary damage, understanding the underlying mechanisms, and adjusting treatment accordingly remain clinically unmet challenges. A significant hallmark of the peri-ischemic brain is a dysfunctional blood–brain barrier (BBB), yet the role of disturbed vascular permeability in stroke progression and for functional outcome is largely unclear.

Here I describe a longitudinal in vivo fluorescence imaging approach for the evaluation of cortical perfusion, BBB dysfunction, free radical formation and cellular injury in the cortical photothrombosis model in male Sprague Dawley rats. In this model light-activated (532 nm) Rose Bengal initiates clot formation thereby preventing sufficient perfusion to the site of illumination. Cerebral perfusion and BBB permeability were quantified from intra- and extravascular distribution kinetics of fluorescein sodium salt following its intravenous bolus application. In parallel, propidium iodide – a membrane integrity marker – served as a cell damage marker and was compared to staining with annexin V, which binds to phosphatidylserin following its exposure on the outer leaflet of the membrane during cellular injury and death. Reactive oxygen and nitrogen species were visualized using ROSstar 650 and 4-amino-5-methylamino-2',7'-difluorofluorescein diacetate and reduced using phenyl-N-t-butylnitrone, L-N^G-nitroarginine methyl ester and carboxy-PTIO.

Imaging the peri-ischemic area demonstrated propagation and progression of hypoperfusion, BBB dysfunction and cell damage during the 3 hour monitoring period following photothrombosis. While hypoperfusion was identified within a belt of ~400 µm surrounding the ischemic core, blood-brain barrier dysfunction and cell damage also occurred at greater distances. Nitric oxide formation most prominently occurred in arterioles, whereas superoxide and hydroxyl radicals gave a diffuse peri-ischemic parenchymal signal. Inhibiting free radical signaling significantly reduced progressive cellular damage after photothrombosis, with no significant effect on blood flow changes and increases in BBB permeability. Of note, cellular injury was only prevented in normally perfused more distant peri-ischemic brain regions (> 400 µm away from the ischemic core). Hence our data is in agreement with previous studies stressing

perfusion based imaging as insufficient to detect tissue at risk. Measurements of BBB permeability could serve as a novel approach to predict lesion progression. In addition, our approach allows a dynamic follow-up of cellular events and their response to therapeutics in the acutely injured cerebral cortex.

Abstract (German)

Schlaganfall ist weltweit eine der Hauptursachen von Morbidität und Mortalität. Ein ischämischer Kern und eine weiter gefasste funktionsgestörte Region, in der es zu sekundärem Zellschaden kommen kann, kennzeichnen dieses Krankheitsbild. Die Anfälligkeit für sekundären Zellschaden zu erfassen, zugrunde liegende Mechanismen herauszufinden und Therapien entsprechend anzupassen, bleiben jedoch Herausforderungen der gegenwärtigen Forschung. Eine eingeschränkte Blut-Hirn-Schranken-Funktion ist im peri-ischämischen Gewebe üblich. Es bleibt jedoch weitgehend unklar, inwieweit diese zur Vergrößerung des Infarktkerns beiträgt und dadurch die klinische Genesung beeinflusst.

In dieser Arbeit beschreibe ich eine longitudinale Methode der in vivo Fluoreszenzbildgebung zur Evaluierung des zerebralen Blutflusses, der Blut-Hirn-Schranken-Permeabilität, der Bildung freier Radikale und des Zelltodes im kortikalen Photothrombosemodell an männlichen Sprague Dawley Ratten. In diesem Modell führt lichtaktiviertes Bengalrosa zur Thrombusformation und verhindert so die ausreichende Blutzufuhr in zuvor illuminiertes Gewebe. Die zerebrale Perfusion und die Blut-Hirn-Schranken-Permeabilität wurden anhand der intra- und extravaskulären Verteilungskinetik von zuvor intravenös injiziertem Fluoresceinsalz quantifiziert. Parallel diente Propidiumjodid, ein Membranintegritätsmarker, als Indikator für Zellschaden. Dieser wurde mit einem zweiten Marker, Annexin V, verglichen. Annexin V bindet an Phosphatidylserin, welches bei Zellschaden und -tod vom Zellinneren an die äußere Lage der Lipiddoppelmembran transloziert wird. Sauerstoff- und Stickstoffradikale wurden durch die Farbstoffe ROSstar 650 und 4-Amino-5-Methylamino-2',7'-Difluorofluorescein-Diacetat sichtbar gemacht, und deren Vorkommen im Gewebe bzw. deren Bildung wurde durch Phenyl-N-t-butylnitron, L-N^G-Nitroargininmethylester und Carboxy-PTIO reduziert.

Das peri-ischämische Gewebe wurde für drei Stunden nach Induktion der Photothrombose bildgebend überwacht. Innerhalb dieses Zeitraums kam es zu Propagation und Progression von Hypoperfusion, Blut-Hirn-Schrankenstörung und Zellschaden. Während hypoperfundiertes Gewebe nur in einem Abstand von ca. 400 µm um den Infarktkern detektiert wurde, war auch weiter entferntes Gewebe von einer Blut-Hirn-Schranken-Störung und Zellschaden betroffen. Stickstoffmonoxid stieg am prominentesten in Arteriolen an, während Superoxid- und Hydroxylradikale ein diffuses

parenchymales peri-ischämisches Signal gaben. Die Blockade freier Radikale reduzierte die Progression von Zellschaden, hatte jedoch weder Einfluss auf die Perfusion noch auf die Blut-Hirn-Schranken-Permeabilität. Interessanterweise wurde die Ausbreitung des Zellschadens nur in normal perfundiertem peri-ischämischem Gewebe (> 400 µm vom Infarktkern entfernt) reduziert. Damit stimmen die Daten mit solchen Studien überein, die betonen, dass perfusionsbasierte Bildgebung nur unzureichend erfasst, ob Gewebe von Sekundärschaden bedroht ist. Messungen der Blut-Hirn-Schrankenpermeabilität könnten als zusätzlicher neuer Ansatz zur Abschätzung der Schadensprogression dienen. Die longitudinale Bildgebung, wie hier im Tiermodell beschrieben, macht es möglich, zelluläre Ereignisse im akut geschädigten Hirngewebe in ihrer Dynamik zu überwachen und den Effekt möglicher Therapeutika zu überprüfen.

Affidavit

I, Karl Schoknecht certify under penalty of perjury by my own signature that I have submitted the thesis on the topic ‘Dynamics and mechanisms of blood-brain barrier dysfunction, cell damage and altered cerebral perfusion after cortical photothrombosis’. I wrote this thesis independently and without assistance from third parties, I used no other aids than the listed sources and resources.

All points based literally or in spirit on publications or presentations of other authors are, as such, in proper citations (see "uniform requirements for manuscripts (URM)" the ICMJE www.icmje.org) indicated. The section on methodology (in particular practical work, laboratory requirements, statistical processing) and results (in particular images, graphics and tables) corresponds to the URM (s.o) and are answered by me. My contribution in the selected publication for this dissertation corresponds to those that are specified in the following joint declaration with the responsible person and supervisor.

The importance of this affidavit and the criminal consequences of a false affidavit (section 156,161 of the Criminal Code) are known to me and I understand the rights and responsibilities stated therein.

Date _____ Signature

Detailed Declaration of Contribution

Karl Schoknecht had the following share in the following publication:

Publication: Schoknecht K, Prager O, Vazana U, Kamintsky L, Harhauses D, Zille M, Figge L, Chassidim Y, Schellenberger E, Kovács, Heinemann U, Friedman A. Monitoring stroke progression: in vivo imaging of cortical perfusion, blood-brain barrier permeability and cellular damage in the rat photothrombosis model. J Cereb Blood Flow Metab. 2014:34/11,1791-80

Contribution in detail: ~75 %, KS designed the study, conducted all but 2 experiments, analysed and interpreted the data, wrote the manuscript and revised the study according to the reviewer’s comments

Signature, date and stamp of the supervising University teacher

_____

Signature of the doctoral candidate

_____

ISI Web of Knowledge℠

Journal Citation Reports®

WELCOME HELP

2013 JCR Science Edition

Journal Summary List

Journal Title Changes

Journals from: subject categories NEUROSCIENCES VIEW CATEGORY SUMMARY LIST

Sorted by: Impact Factor SORT AGAIN

Journals 1 - 20 (of 252) [1 | 2 | 3 | 4 | 5 | 6 | 7 | 8 | 9 | 10] Page 1 of 13

MARK ALL UPDATE MARKED LIST

Ranking is based on your journal and sort selections.

Mark	Rank	Abbreviated Journal Title (linked to journal information)	ISSN	JCR Data						*Eigenfactor*® Metrics	
				Total Cites	Impact Factor	5-Year Impact Factor	Immediacy Index	Articles	Cited Half-life	*Eigenfactor*® Score	*Article Influence*® Score
☐	1	NAT REV NEUROSCI	1471-003X	30120	31.376	37.472	6.161	62	6.9	0.08887	16.773
☐	2	ANNU REV NEUROSCI	0147-006X	13345	22.660	28.613	1.542	24	>10.0	0.02776	15.009
☐	3	TRENDS COGN SCI	1364-6613	18076	21.147	18.920	2.983	60	7.9	0.04375	8.363
☐	4	NEURON	0896-6273	71989	15.982	16.485	2.902	369	8.1	0.22596	8.682
☐	5	MOL PSYCHIATR	1359-4184	13902	15.147	14.196	3.500	132	5.4	0.03924	4.672
☐	6	NAT NEUROSCI	1097-6256	46095	14.976	16.273	3.725	236	7.4	0.15123	8.604
☐	7	BEHAV BRAIN SCI	0140-525X	7017	14.962	22.821	4.476	21	>10.0	0.00965	10.342
☐	8	TRENDS NEUROSCI	0166-2236	18523	12.902	14.345	2.534	73	9.9	0.03683	6.407
☐	9	ANN NEUROL	0364-5134	33670	11.910	11.353	1.893	178	9.5	0.06302	4.184
☐	10	PROG NEUROBIOL	0301-0082	11310	10.301	10.570	1.745	51	9.1	0.02116	3.480
☐	11	NEUROSCI BIOBEHAV R	0149-7634	15111	10.284	11.075	1.401	207	6.7	0.03829	3.731
☐	12	BRAIN	0006-8950	44457	10.226	10.846	2.125	272	8.2	0.08991	3.874
☐	13	ACTA NEUROPATHOL	0001-6322	12284	9.777	8.854	2.717	120	6.5	0.03087	3.082
☐	14	BIOL PSYCHIAT	0006-3223	40687	9.472	10.347	2.883	239	7.4	0.08145	3.332
☐	15	SLEEP MED REV	1087-0792	3512	9.141	9.320	2.186	43	6.2	0.00917	3.201
☐	16	CEREB CORTEX	1047-3211	24708	8.305	8.372	2.410	268	6.3	0.07654	3.462
☐	17	NEUROPSYCHOPHARMACOL	0893-133X	21567	7.833	8.518	1.765	255	6.0	0.05741	2.820
☐	18	J PINEAL RES	0742-3098	6136	7.812	5.961	2.011	88	5.9	0.00750	0.919
☐	19	NEUROSCIENTIST	1073-8584	3594	7.618	6.491	1.702	47	6.6	0.00915	2.367
☐	20	FRONT NEUROENDOCRIN	0091-3022	3070	7.581	10.579	1.160	25	5.4	0.00934	3.419

Journal Summary List

Journal Title Changes

Journals from: subject categories NEUROSCIENCES VIEW CATEGORY SUMMARY LIST

Sorted by: Impact Factor SORT AGAIN

Journals 21 - 40 (of 252) [1 | 2 | 3 | 4 | 5 | 6 | 7 | 8 | 9 | 10] **Page 2 of 13**

MARK ALL UPDATE MARKED LIST

Ranking is based on your journal and sort selections.

Mark	Rank	Abbreviated Journal Title (linked to journal information)	ISSN	JCR Data						*Eigenfactor*® Metrics	
				Total Cites	Impact Factor	5-Year Impact Factor	Immediacy Index	Articles	Cited Half-life	*Eigenfactor*® Score	*Article Influence*® Score
☐	21	J PSYCHIATR NEUROSCI	1180-4882	2519	7.492	7.234	1.105	38	5.5	0.00657	2.143
☐	22	HUM BRAIN MAPP	1065-9471	14858	6.924	6.956	1.315	257	6.0	0.04166	2.440
☐	23	CURR OPIN NEUROBIOL	0959-4388	12062	6.765	7.549	1.701	147	8.1	0.03586	4.031
☐	24	J NEUROSCI	0270-6474	167915	6.747	7.648	1.232	1765	7.7	0.41315	3.058
☐	25	NEURON GLIA BIOL	1740-925X	561	6.636	3.868		0	5.8	0.00161	1.269
☐	26	NEUROIMAGE	1053-8119	69654	6.132	6.956	1.479	873	6.2	0.17268	2.214
☐	27	BRAIN BEHAV IMMUN	0889-1591	7365	6.128	5.813	1.389	185	4.5	0.02120	1.657
☐	28	CORTEX	0010-9452	5977	6.042	5.389	1.266	252	5.7	0.01474	1.685
☐	29	BRAIN RES REV	0165-0173	8452	5.930	8.781		0	9.0	0.01313	2.975
☐	30	SOC COGN AFFECT NEUR	1749-5016	2787	5.884	6.447	1.957	117	3.5	0.01209	2.403
☐	31	PAIN	0304-3959	30877	5.836	6.341	1.084	323	9.2	0.04899	1.937
☐	32	CURR OPIN NEUROL	1350-7540	5005	5.729	5.365	0.957	92	5.8	0.01477	1.902
☐	33	PSYCHONEUROENDOCRINO	0306-4530	10669	5.591	6.090	0.893	318	5.8	0.02392	1.691
☐	34	MOL AUTISM	2040-2392	335	5.486	6.080	0.644	45	2.4	0.00180	2.159
☐	35	GLIA	0894-1491	10995	5.466	5.374	1.631	157	7.0	0.02247	1.675
☐	36	BRAIN STIMUL	1935-861X	1502	5.432	6.950	0.822	129	3.0	0.00634	1.911
☐	37	NEUROPSYCHOL REV	1040-7308	1914	5.400	7.672	0.700	20	5.6	0.00551	2.526
☐	38	EUR NEUROPSYCHOPHARM	0924-977X	4652	5.395	4.736	0.773	185	5.5	0.01103	1.314
☐	39	J CEREBR BLOOD F MET	0271-678X	14721	5.339	5.373	0.923	233	8.0	0.02875	1.755
☐	40	MOL NEUROBIOL	0893-7648	3261	5.286	5.843	1.219	169	4.9	0.00838	1.716

Journal of Cerebral Blood Flow & Metabolism (2014) 34, 1791–1801

www.jcbfm.com

ORIGINAL ARTICLE

Monitoring stroke progression: *in vivo* imaging of cortical perfusion, blood–brain barrier permeability and cellular damage in the rat photothrombosis model

Karl Schoknecht[1], Ofer Prager[2], Udi Vazana[2], Lyn Kamintsky[2], Denise Harhausen[3], Marietta Zille[3], Lena Figge[4], Yoash Chassidim[2], Eyk Schellenberger[4], Richard Kovács[1], Uwe Heinemann[1] and Alon Friedman[2,5]

Focal cerebral ischemia is among the main causes of death and disability worldwide. The ischemic core often progresses, invading the peri-ischemic brain; however, assessing the propensity of the peri-ischemic brain to undergo secondary damage, understanding the underlying mechanisms, and adjusting treatment accordingly remain clinically unmet challenges. A significant hallmark of the peri-ischemic brain is dysfunction of the blood–brain barrier (BBB), yet the role of disturbed vascular permeability in stroke progression is unclear. Here we describe a longitudinal *in vivo* fluorescence imaging approach for the evaluation of cortical perfusion, BBB dysfunction, free radical formation and cellular injury using the photothrombosis vascular occlusion model in male Sprague Dawley rats. Blood–brain barrier dysfunction propagated within the peri-ischemic brain in the first hours after photothrombosis and was associated with free radical formation and cellular injury. Inhibiting free radical signaling significantly reduced progressive cellular damage after photothrombosis, with no significant effect on blood flow and BBB permeability. Our approach allows a dynamic follow-up of cellular events and their response to therapeutics in the acutely injured cerebral cortex.

Journal of Cerebral Blood Flow & Metabolism (2014) **34,** 1791–1801; doi:10.1038/jcbfm.2014.147; published online 27 August 2014

Keywords: blood–brain barrier; brain imaging; cell death mechanisms; cerebral blood flow; focal ischemia

INTRODUCTION

Focal ischemic stroke is among the main causes of death and morbidity worldwide.[1] Thrombolytic therapy remains the only approved treatment for acute ischemic stroke, yet it only benefits a limited number of patients diagnosed and treated within the first few hours after the insult.[2,3] Patients' outcome was shown to be critically determined by alterations in the brain tissue surrounding the ischemic core; for example, in the vicinity of the lesion core, nonischemic brain regions are often characterized by reduced blood flow and disturbed neural functions.[4] Recent studies pointed to vascular dysfunction, specifically impairment in blood–brain barrier (BBB) permeability as an additional important hallmark of the peri-ischemic brain.[5] Indeed, changes directly related to BBB opening seem to play a critical role in the pathogenic process after stroke. Kuntz *et al*[6] recently showed BBB dysfunction coinciding with cell damage in a cell culture model of ischemia and reperfusion, and after transient medial cerebral artery occlusion in mice. Experimental BBB injury in rodents leads to neuronal dysfunction, spreading depolarization, seizures and delayed degeneration—all well-known complications of stroke.[7–11] In stroke patients, BBB dysfunction is associated with increased risk of secondary hemorrhage and cerebral edema, further compromising perfusion because of vasospasms or through increased intracranial pressure.[2,7,12,13] However, the spatiotemporal dynamics and mechanisms underlying vascular alterations and the potential link between BBB opening, neurovascular dysfunction and cellular injury after stroke are not fully understood.

We studied photothrombosis (PT)-induced changes in cortical perfusion, BBB permeability, free radical formation and cell injury *in vivo*—focusing on the longitudinal experimental design to allow a parallel study of the spatiotemporal dynamics of these parameters. Cortical perfusion and BBB permeability were quantified using fluorescent angiography by intravenous application of fluorescein sodium salt, commonly used in the clinics to assess retinal blood flow and blood–retinal barrier permeability;[14] in these studies the first pass of the tracer bolus (representing vascular filling) is used to determine tissue perfusion and the delayed extravascular (EV) accumulation of the tracer reflects its leakage from injured vessels.[15–17] Formation of reactive oxygen and nitrogen species were monitored using different fluorescent probes. Nitric oxide (NO) was detected using 4-amino-5-methylamino-2′,7′-difluorofluorescein diacetate (Molecular Probes, Eugene, OR, USA; its oxidative derivatives being reactive with NO) as

[1]Institute for Neurophysiology, Charité—University Medicine Berlin, Berlin, Germany; [2]Departments of Physiology and Cell Biology, Cognitive and Brain Sciences, The Zlotowski Center for Neuroscience, Ben-Gurion University of the Negev, Beer-Sheva, Israel; [3]Department of Experimental Neurology, Center for Stroke Research Berlin (CSB), Charité—University Medicine Berlin, Berlin, Germany; [4]Department of Radiology, Charité—University Medicine Berlin, Berlin, Germany and [5]Department of Medical Neuroscience, Faculty of Medicine, Dalhousie University, Halifax, Canada. Correspondence: Professor A Friedman, Dennis Chair in Epilepsy Research, Department of Medical Neuroscience, Faculty of Medicine, Dalhousie University, Halifax B3H 4R2, Canada.
E-mail: alon.friedman@dal.ca
This work was supported by the TSB Technologiestiftung Berlin—Zukunftsfonds Berlin, cofinanced by the European Union—European fund for regional development, the Bundesministerium für Bildung und Forschung (BMBF), the German Research Foundation (Cluster of Excellence DFG-EXC 257 NeuroCure and DFG He 1128/18-1), the Herman and Lilly Schilling Foundation, and the European Union's Seventh Framework Programs (FP7/2008-2013) under grant agreements no. 201024 and no. 202213 (European Stroke Network) and no. 602102 (EPITARGET)
Received 30 April 2014; revised 15 July 2014; accepted 21 July 2014; published online 27 August 2014

previously used in a transient medial cerebral artery occlusion model in mice,[18] and reactive oxygen species (superoxide and hydroxyl radicals) were detected by ROSstar 650 (Li-Cor, Lincoln, NE, USA), a hydrocyanine-based indicator, previously used *in vivo* after lipopolysaccharide-induced peritoneal inflammation and implant-associated inflammation.[19,20] ROSstar 650 (Li-Cor) is membrane permeable in its reduced form and becomes fluorescent and membrane impermeable once oxidized, hence can be used for the detection of intracellular reactive oxygen species (ROS) formation.[19] Cellular injury was detected using propidium iodide (PI), a membrane integrity marker that binds to DNA/RNA and increases its fluorescence by a factor of 20 to 30 upon binding, and fluorescently labeled annexin V, an endogenous protein with high affinity to phosphatidylserine. Phosphatidylserine becomes exposed to the outer leaflet of the membrane during apoptosis and necrosis and has been successfully detected in animal models of cerebral ischemia and in a human study.[21,22] As ROS were shown to be involved in deleterious processes within the peri-ischemic brain,[23–25] we aimed to use our imaging approach to follow the spatial and temporal progression of ROS synthesis after the insult. This approach enabled us to test the modifying effect of inhibiting free radical signaling on the dynamics of cortical perfusion, BBB permeability and cell damage in the peri-ischemic brain.

MATERIALS AND METHODS

All experimental procedures were performed according to the guidelines of the animal care and ethical committee at Ben-Gurion University of the Negev, Beer-Sheva, Israel.

Photothrombosis Model of Vascular Occlusion

A total of 34 male Sprague Dawley rats (bodyweight 235 to 380 g, Harlan, Jerusalem, Israel), housed under standard conditions with free access to food and water, underwent craniotomy over the right somatosensory cortex (2 mm frontal—4 mm occipital and 2 to 6 mm lateral to bregma) under deep anesthesia (intraperitonal injection of ketamine (100 mg/mL, 0.08 mL/100 g) and xylazine (20 mg/mL, 0.06 mL/100 g)).[16] Oxygen saturation was continuously monitored at the hind paw (Starr Life Science MouseOx probe, Oakmont, PA, USA) and body temperature was kept at 37°C ± 0.5 °C using a heating pad. After removal of the dura, Rose bengal (RB, Sigma-Aldrich, St Louis, MO, USA) was injected into the tail vein (0.133 mL/ 100 g bodyweight, 7.5 mg/mL saline, 9.8 μmol/l/kg) and PT was induced using focal illumination (532 nm, diameter of ~1 mm, CNI Laser, MGL-III-532-5 mW-1.5, Changchun, China) for 15 minutes.[26] The animal was strictly shielded from light, minimizing diffuse RB activation after laser illumination.

Intravital Fluorescence Imaging

The imaging-setup consisted of a fluorescence microscope (Zeiss SteReO Lumar V12; Oberkochen, Germany) with three built-in filters and an EMCCD camera (Andor Technology, DL-658 M-TIL; Belfast, UK). Images were captured at x6.4 to x40 magnification with quantitative analysis based on x30 magnification and a region of interest of 2.19 mm × 1.65 mm. Perfusion and BBB permeability assessment were based on intravenous injections of fluorescein sodium salt (1 mg/kg bodyweight, 1 mg/mL saline, Sigma-Aldrich, St Louis, MO, USA) pre-PT and hourly after PT. Images were taken at 5 Hz for 306 seconds starting 6 seconds before injection. To detect cell death/damage, recombinant human annexin A5 (from Chris P Reutelingsperger) was labeled with fluorescein isothiocyanate (FITC, Sigma-Aldrich, St Louis, MO, USA) as described.[27] Two forms were used: annexin A5 with retained affinity for phosphatidylserine and nonbinding annexin A5 with a complete loss of affinity for phosphatidylserine. Both FITC-labeled annexin A5 preparations were diluted in saline from FITC annexin stock (nonbinding: 1 g/l protein, cFITC 22.2 μmol/l, FITC/annexin ratio 0.8; binding: 1.2 g/l protein, cFITC 20.5 μmol/l, FITC/annexin ratio 0.6) and ~25 nmol of FITC/100 g bodyweight were injected intravenously into the tail vein before and after PT ($n = 4$). Propidium iodide (Molecular Probes, Eugene, OR, USA; 0.5 mg/kg bodyweight, 0.5 mg/ml saline) was intravenously injected before and hourly after PT or superfused topically. Topical application of PI, to bypass the BBB, did not prove feasible as widespread surface noise was always detected ($n = 4$, data not shown). Propidium iodide and FITC-annexin A5 signals were acquired before tracer injection and 10 minutes after injection at 1 Hz. For quantitative image analysis of PI, an averaged image (consisting of 10 frames) was created.

ROSstar 650 (Li-Cor) to detect superoxide and hydroxyl radicals was applied by intravenous injection (0.2 to 0.5 mL saline-based solution, concentration: 50 to 100 μmol/l) 30 minutes before the induction of PT and reinjected up to 90 minutes after RB injection ($n = 2$) or was topically applied and incubated for 30 minutes before imaging ($n = 1$). 4-Amino-5-methylamino-2′,7′-difluorofluorescein diacetate (Molecular Probes) was topically applied (concentration: 50 to 200 μmol/l, 30 minutes incubation)[18] before PT for baseline imaging and ~3 hours after PT to detect NO ($n = 5$).

For BBB imaging in deep cortical layers *ex vivo*, 0.2 mL/ 100 g bodyweight of 2% Evans blue solution (Sigma-Aldrich, St Louis, MO, USA) was injected into the tail vein 1 hour before sacrificing the animal as previously reported.[8,28,29]

Inhibition of Reactive Oxygen Species

To inhibit reactive oxygen/nitrogen species and their generation, a combination of 1 mmol/l 2-(4-carboxyphenyl)-4,4,5,5-tetramethyl-imidazoline-l-oxyl-3-oxide (carboxy-PTIO, NO scavenger; Tocris, Bristol, UK), 1 mmol/l L-N^G-Nitroarginine methyl ester (NO synthase inhibitor; Tocris, Bristol, UK) and 1 mmol/l phenyl-*N*-t-butylnitrone (free radical spin trap (superoxide) and inhibitor of induction of NO synthase; Sigma-Aldrich, St Louis, MO, USA) were used and perfused in artificial cerebrospinal fluid. Animals were assigned randomly to the treatment group ($n = 9$). In the nontreated group ($n = 9$), two animals were excluded because of BBB opening before PT induction. Since the PT model is based on free radical generation (by activated RB), and to ensure that free radical inhibiting treatment will not affect clot generation and development of the ischemic core, we started topical perfusion (0.5 ml/h) with free radical inhibitors 30 minutes after RB injection when >90% of blood RB was hepatically eliminated.[30]

Ex Vivo Microscopy and Histology

Snap-frozen brains were cut in 20 μm thick coronal slices with a cryostat (Leica CM 1950, Wetzlar, Germany) and rinsed in an alcohol series of decreasing concentrations before incubation with hemalaun (Merck, Darmstadt, Germany). The slices were then rinsed in 96% ethanol with 2% hydrochloric acid and incubated in 2% sodium bicarbonate. After dehydration and mounting, the sections were analyzed with a LEICA DMRE microscope (Leica Microsystems Jena Gmbh, Jena, Germany). For detection of annexin A5 and PI signals, *ex vivo* nonstained adjacent slices were used.

Data Processing and Analysis

Imaging data were transferred to MATLAB and corrected for movement artifacts as described.[16] To estimate relative perfusion, we first extracted the arterial input function (AIF, dynamic arterial signal intensity after tracer injection) from an arteriole (at least one branching point away from the occluded vessel) that stayed perfused throughout the experiment as documented by repeated fluorescent angiography. The ratio between the maximal intensity change in each pixel during first pass (FP_Max) and the maximal AIF (maxAIF) was termed 'relative perfusion' and taken as a surrogate marker for local cerebral perfusion. The 'lesion border' was defined by post PT angiography, which delineated the ischemic core, where arteriolar supply was blocked, from the peri-ischemic brain. For each pixel relative perfusion was presented as a function of distance from this border. Averaged relative perfusion values were calculated for pixels in eccentric rings of 100 μm width starting at the lesion border and normalized to the control value measured before PT (normalized relative perfusion = (FP_Max(PT)/maxAIF(PT))/(FP_Max(Pre PT)/maxAIF(Pre PT)) × 100%). To quantify the area most severely affected by reduced perfusion, we arbitrarily set a perfusion threshold at 30% maxAIF during tracer first pass. Although >99% of the pixels were above threshold in the intact brain, thus identified as 'normally perfused', the majority of pixels within the ischemic core (70.0% ± 12.0%) were characterized as 'hypoperfused' according to this threshold.

To assess vascular permeability, the EV and vascular compartment were segmented on the basis of an arteriovenous first-pass overlay image and the 'adaptive threshold' function in MATLAB.[29] For each EV pixel, the integral of the decay phase of the postinjection curve was computed and divided by the AIF integral (EV/AIF), thereby comparing the change in EV signal intensity (reflecting tracer accumulation) relative to the arterial

input. We refer to this ratio as the 'BBB permeability index'. Cellular damage was quantified as the number of PI-positive pixels after background correction. Both BBB permeability and cell damage were assessed as functions of distance to the lesion border (as described above).

Statistical Analysis

Statistical analysis was performed with nonparametric Friedman's analysis of variance for related samples and nonparametric Mann–Whitney *U*-test for independent samples with Bonferroni *post hoc* correction. Differences were considered significant at $P < 0.05$. All statistical analyses were performed with SPSS v.20.0 (IBM Corporation, Armonk, NY, USA). Data is shown as mean ± s.e.m.

RESULTS

Photothrombosis was induced through simultaneous RB injection and laser illumination, impairing blood flow within seconds

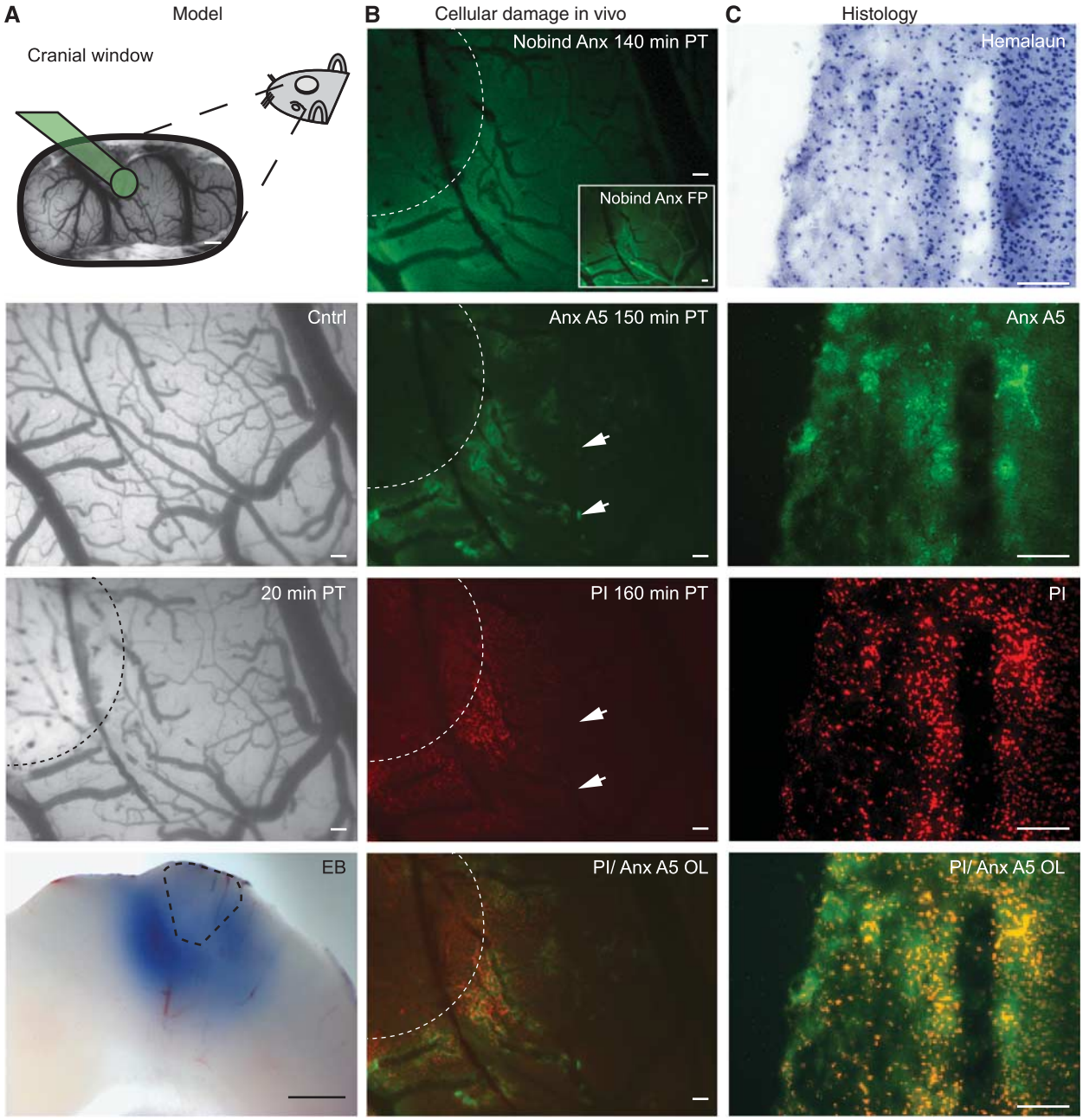

Figure 1. Photothrombosis model description and evaluation of cell damage markers. From top to bottom: (**A**) representative preparation of the cranial window. Green cone projects to area undergoing photothrombosis (PT). Pial vasculature pre- and post Rose bengal-induced PT. Dotted line marks area that was illuminated by the green laser. Evans blue (EB) extravasation (bottom) indicates blood–brain barrier dysfunction on the brain's surface as well as in deep cortical layers *ex vivo*. Dotted line estimates lesion core. (**B**) Intravital microscopy revealed no specific staining with nonbinding annexin A5 (Nobind Anx A5) 140 minutes after PT. Presence of the protein, however, was confirmed during bolus first pass (FP, see inset). Binding annexin A5 (Anx A5) was found in perilesional brain parenchyma 150 minutes after PT injection, mainly in close proximity to venules. Propidium iodide (PI) stained damaged cells surrounded the lesion 160 minutes after PT. Overlay of Anx A5 and PI confirmed costaining of Anx A5-positive parenchyma with PI. Note also Anx A5-positive and PI-negative regions (arrowheads) indicating potentially reversible cell damage. (**C**) Hemalaun staining and Anx A5, PI and Anx A5/PI overlay as detected *ex vivo*. Scale bar = 500 μm in A top and A bottom, all others 100 μm.

(see Supplementary Movie). Consistent with previous studies, macroscopic sections confirmed BBB breakdown in most layers of the cortex surrounding the lesion core (Figure 1A, bottom).[8,28,29] Cellular damage was detected in the peri-ischemic region using intravital microscopy after intravenous injection of either PI or binding annexin A5, while nonbinding annexin A5 gave no specific staining (Figure 1B). Positive annexin A5 staining, while generally colocalized with PI ($n = 4$), was most prominent in close proximity to blood vessels, mainly venules. Notably, in the periphery of the peri-ischemic regions, positive annexin A5 staining was not always associated with PI fluorescence (Figure 1B, arrows). Similar to BBB dysfunction (Figure 1A, bottom), *ex vivo* microscopy confirmed cellular injury in most cortical layers (Figure 1C). For quantitative analysis of cell injury we used PI images, since PI gave a better signal to noise ratio compared with annexin, perhaps because of its small molecular size and rapid diffusion or because of increased fluorescence upon DNA/RNA binding.[31]

Using repeated angiography, we quantified dynamic changes in relative perfusion within each treated brain, allowing the characterization of three regions: (1) an 'ischemic core'—where PT was induced and arterial supply permanently blocked; (2) an *adjacent peri-ischemic zone* with significantly reduced blood flow compared with the pre-PT state ($< 400\,\mu$m); and (3) a *distant peri-ischemic zone*—in which perfusion was intact (similar to pre-PT state) throughout the 3 hour monitoring period (Figure 2).

Longitudinal *in vivo* imaging showed that reduction in perfusion, increased vascular permeability, and cellular damage clearly progressed within the peri-ischemic brain after PT (Figures 2C–F, Figure 3). Notably, while reduced blood flow was limited to the adjacent peri-ischemic zone, BBB permeability and cell damage (PI signal) were increased within both the adjacent and distant peri-ischemic region (Figures 3B–D, see quantification below and Figure 6).

To study the involvement of free radical signaling in the peri-ischemic brain, we monitored the formation of NO (using 4-amino-5-methylamino-2′,7′-difluorofluorescein (DAF-FM) diacetate), and of superoxide and hydroxyl radicals (using ROSstar 650 (Li-Cor)) *in vivo*. Oxidized ROSstar 650 (Li-Cor) and the NO-adduct of DAF-FM diacetate were detected in the ischemic core and within the peri-ischemic cortex (Figures 4 and 5). Although PT was followed by a diffuse vascular and parenchymal signal of ROSstar 650 (Li-Cor; $n = 3$; Figure 4), NO staining delineated arterioles ($n = 5$, Figures 5C and 5D). The delayed detection of free radicals in the peri-ischemic brain suggests that free radical formation was independent of direct RB activation. We further investigated whether inhibition of ROS signaling affected cerebral perfusion, BBB permeability, and cell damage after PT by applying a 'cocktail' containing phenyl-*N*-t-butylnitrone (free radical spin trap), L-N^G-nitroarginine methyl ester (NO synthetase inhibitor), and carboxy-PTIO (NO scavenger) 30 minutes after PT. We applied this cocktail, rather than selective blockers, because reactive oxygen as well as nitrogen species (especially peroxynitrite) were shown to be involved in the no-reflow phenomenon after medial cerebral artery occlusion,[25] and in cellular damage.[23,24]

Quantitative analysis of relative perfusion, BBB permeability, and cellular injury with and without ROS inhibition (treatment: $n = 9$; no treatment: $n = 7$) confirmed lesion progression in the PT model. Without treatment, $11.3\% \pm 2.9\%$ of the adjacent zone was hypoperfused (below 30% maximal AIF, $P = 0.04$) 1 hour after clot formation, and $25.1\% \pm 4.4\%$ was hypoperfused after 3 hours (Figure 6A, $P < 0.001$). No significant perfusion deficit was observed in the distant peri-ischemic zone. Reactive oxygen species inhibition reduced the percentage of hypoperfused tissue in the adjacent zone to $4.8\% \pm 1.4\%$ and $13.2\% \pm 3.1\%$ at 1 and 3 hours after PT, respectively, however not reaching significance ($P = 0.102$ and 0.041, respectively before *post hoc* correction; Figure 6A).

Vascular permeability to the injected sodium fluorescein was significantly increased in the adjacent zone one hour after PT ($11.11\% \pm 1.88\%$, $P < 0.001$) and propagated to the distant peri-ischemic region (2.9 ± 1.76, $P = 0.01$) at 3 hours. ROS inhibition had no effect on the progression of BBB permeability changes (Figure 6B).

Quantitative analysis of the PI signal confirmed propagation of PT-induced cellular damage within the peri-ischemic brain (Figure 6C). The number of PI-positive pixels significantly increased within the adjacent peri-ischemic region when observed 1 hour after PT ($2.7\% \pm 1.1\%$ versus $0.002\% \pm 0.002\%$, post- versus pre-PT, respectively, $P = 0.003$). After 3 hours, PI signal was significantly increased in both the adjacent ($17.2\% \pm 2.6\%$ PI-positive pixels, $P < 0.001$) and distant zone ($4.9\% \pm 1.6\%$ versus $0.9\% \pm 0.5\%$ PI-positive pixels, post- versus pre-PT, $P = 0.002$; Figure 6C). Although cellular injury in the adjacent zone remained unaffected by ROS inhibition, the treatment effectively prevented the progression of cellular damage to the distant peri-ischemic region, where cellular damage was significantly reduced to $0.3\% \pm 0.2\%$ of PI-positive pixels ($P < 0.001$, Figure 6C).

DISCUSSION

Using longitudinal *in vivo* imaging within individual animals, we monitored the progressive nature of lesion development after clot formation. During the first 3 hours after PT we show (1) a progressive reduction in blood flow, BBB dysfunction, and cellular damage in the peri-ischemic brain; (2) progression of BBB breakdown and cell damage exceeding the hypoperfused brain areas; (3) synthesis of reactive oxygen species within the lesion core and its surroundings; and (4) reduced progression of cell damage into the distant perilesional zone under inhibition of free radical signaling, without significant effects on changes in perfusion and permeability.

The classic stroke literature describes an ischemic core and a surrounding brain region of dysfunctional brain parenchyma with reduced perfusion that may escape cell death (referred to as 'benign oligemia') or may undergo delayed infarction (true 'tissue-at-risk').[4,32] However, defining thresholds and measuring levels of cerebral perfusion to distinguish regions with 'benign oligemia' from true 'tissue-at-risk' remains challenging. This is not only because of the limitations of available imaging modalities (mainly computed tomography and magnetic resonance imaging

Figure 2. Partitioning the peri-ischemic brain according to perfusion measurements. (**A**) Schematic of the ischemic core (IC), the adjacent (AZ), and distant peri-ischemic zone (DZ, lesion border, LB). (**B**) Flow curves, taken from the fluorescent angiography illustrate reduced perfusion in AZ and IC, while the reference arteriole (AIF, arterial input function) and DZ remained unaffected. PT, photothrombosis. (**C**) Relative perfusion maps by pixel-based normalization of the first pass maximum (FP_Max, see B) to the maximal AIF (maxAIF). (**D**) Relative perfusion averaged by distance to LB. (**E**) Relative perfusion normalized to pre-PT perfusion calculated as follows: ##normalized relative perfusion = (FP_Max(PT)/maxAIF (PT))/(FP_Max(Pre PT)/maxAIF(Pre PT)) × 100%. (**F**) Quantitative analysis reveals that reduced normalized relative perfusion remains within 400 μm from LB during the 3 hours monitoring period ($n = 7$) allowing the division of the peri-ischemic brain into AZ and DZ. For statistical analysis nonparametric paired Friedman's analysis of variance including Bonferroni *post hoc* correction was performed; adjusted *P*-values in control comparison ***$P < 0.001$; **$P < 0.01$; *$P < 0.05$. Data shown as mean ± s.e.m. #For graphical simplicity only largest distance shown on axis label (e.g., '200' contains mean of all values between 100 and 200 μm); scale bar = 200 μm.

perfusion), e.g., utilizing nonuniform image processing,[33] but also because of the dynamic nature of stroke pathophysiology itself resulting in varying viability thresholds at different time points after stroke.[32] In our study, regional differences in cerebral perfusion were measured using fluorescent angiography, previously shown to correlate with laser Doppler flowmetry.[16,29] Angiography

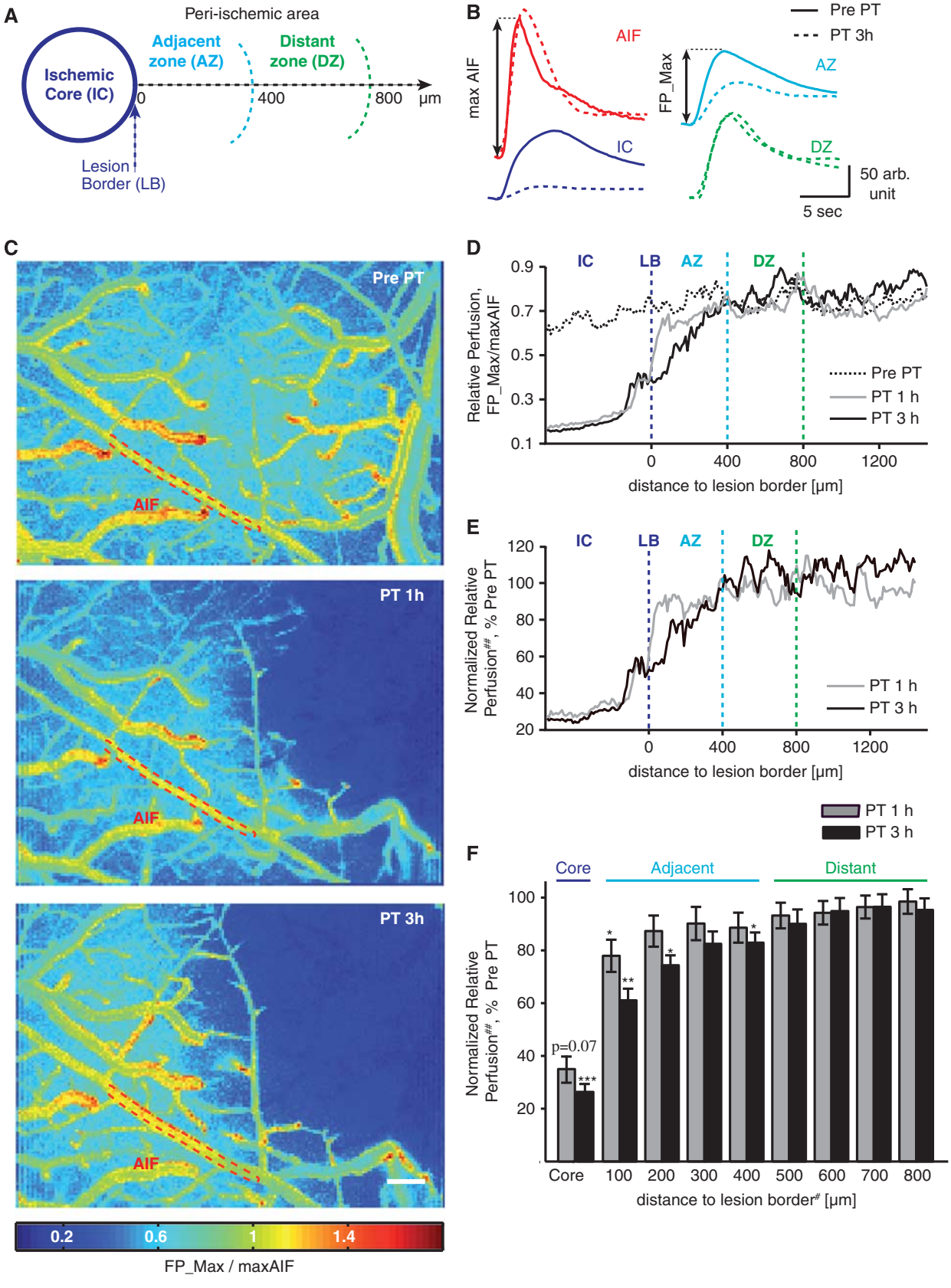

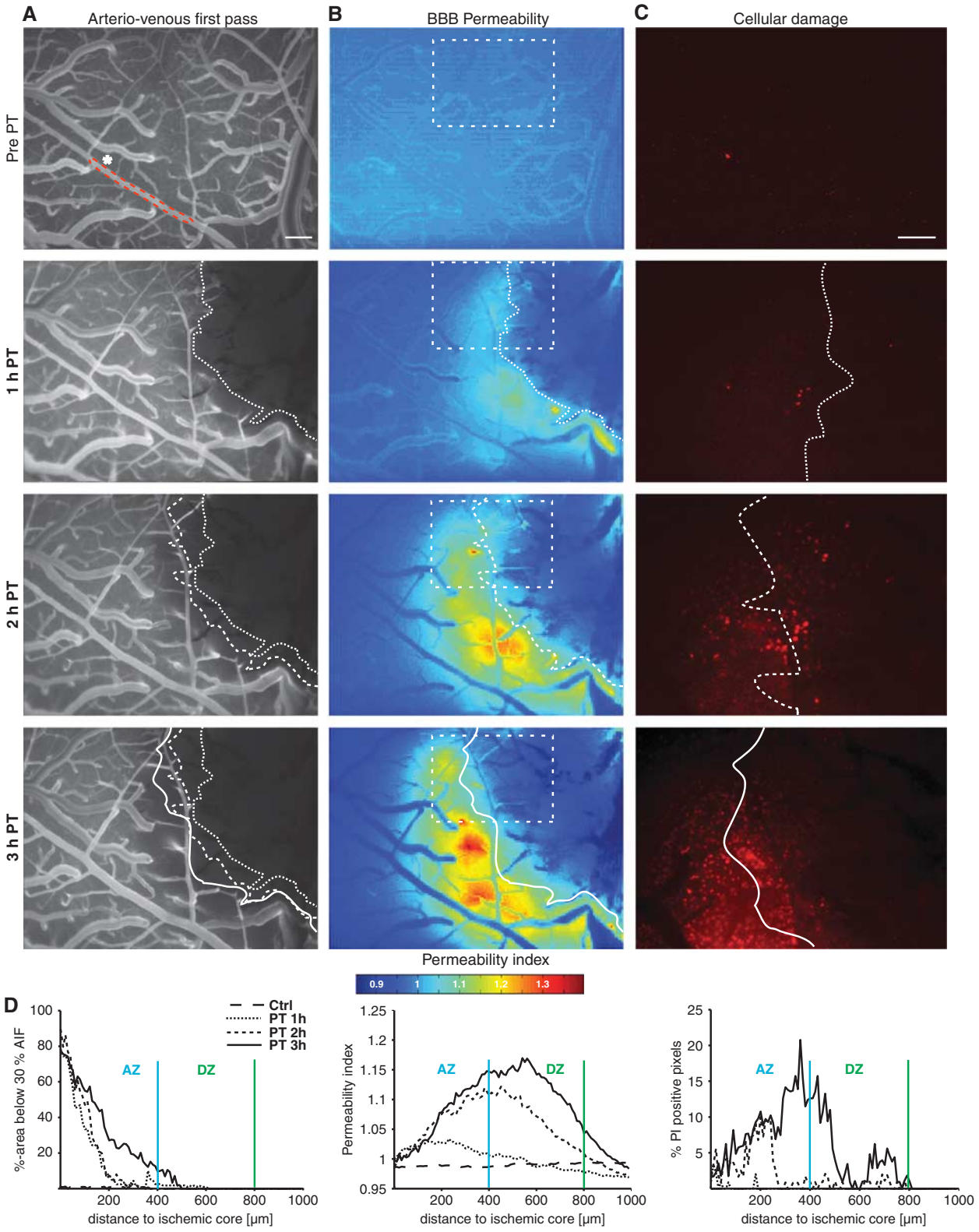

Figure 3. Parallel intravital monitoring of relative cerebral perfusion, blood–brain barrier (BBB) permeability, and cell damage. (**A**–**C**) From top to bottom: images under control condition and 1 to 3 hours after Rose bengal-induced photothrombosis. (**A**) Arteriovenous first pass images. Pixels were counted as hypoperfused when below a threshold of 30% of the maximum of the arterial input function (AIF—selected arteriole marked by asterisk and red dotted line). The white dotted line marks the hypoperfused lesion core. (**B**) BBB permeability maps. Dotted square marks region of interest shown in C. Dotted lines were transferred from A. (**C**) Cell damage as detected by propidium iodide (PI). Note how cell damage progresses into normally perfused perilesional brain tissue. Increases in BBB permeability seem to precede cell damage. (**D**) The graphs show how hypoperfusion, increased BBB permeability, and cell damage affected growing perilesional areas with time after PT. AZ, adjacent zone; DZ, distant zone. Scale bar = 200 μm.

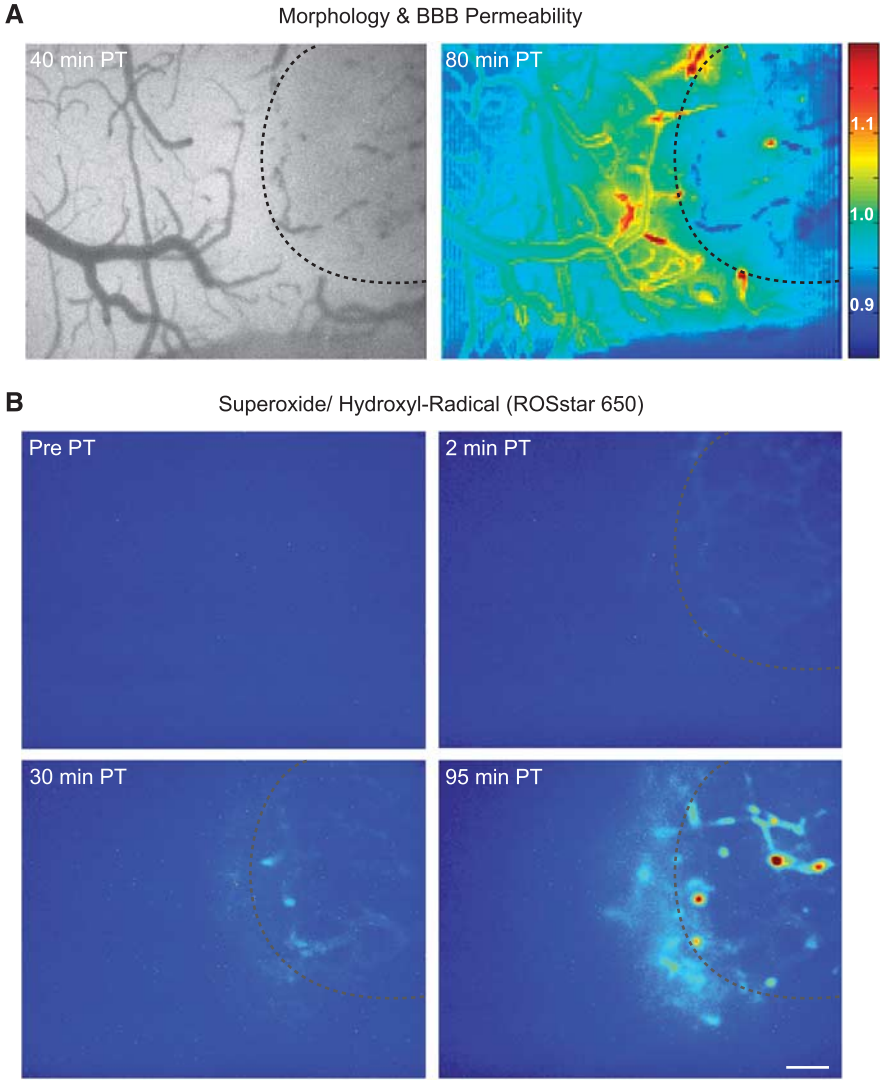

Figure 4. Intravital microscopy reveals superoxide and hydroxyl radical formation after photothrombosis (PT). (**A**) Left: bright field image 40 minutes after PT induction. Right: blood–brain barrier (BBB) permeability index 80 minutes after PT. (**B**) Areas with enhanced superoxide and hydroxyl radical formation. Note the detection of free radicals in the ischemic core as well as in the peri-ischemic cortex. (**A** and **B**) Dotted lines indicate previously laser-illuminated ischemic core. Scale bar = 200 μm.

allows measuring blood flow in a higher spatial, yet limited temporal resolution compared with laser Doppler flowmetry. Most importantly, using this technique, we were able to quantify changes in vascular permeability owing to leakage of tracer through the dysfunctional BBB.[16,34] We describe an ischemic core (~1.2 mm diameter) surrounded by a rim with a width of ~ 400 μm that was characterized by progressive hypoperfusion and cell damage during the 3 hours of monitoring. This region is consistent with the small peri-ischemic hypoperfused rim described 1 to 6 hours after stroke in patients, that may predict tissue deterioration.[35]

We used intravenous annexin A5 and PI to follow cellular damage *in vivo*, as these were previously shown to increase in models of brain injury and confirmed by terminal transferase-mediated dUTP nick-end labeling costaining *ex vivo*.[21,22,36] Although PI, as a marker for membrane integrity, is assumed to detect irreversible damage, phosphatidylserine exposure was shown to be reversible under mild stress. Hence annexin A5-positive cells may potentially escape cell death.[37] We saw a large overlap between PI and annexin A5 staining in the peri-ischemic brain. In an earlier study using the PT model, the largest fraction of apoptotic cells surrounding the infarct core were morphologically identified as neurons.[38] Similarly, Van Hoecke *et al*[39] describe a 'surrounding pale region' around the ischemic core characterized by significant neuronal cell death forming within the first 12 to 24 hours after PT. Conversely, resident microglia, blood-borne leukocytes and astrocytes start to align and proliferate around the lesion core within the first 24 to 48 hours.[40,41] Interestingly, within the periphery of the peri-ischemic zone we detected annexin A5-positive, PI-negative cells, suggesting reversible cellular injury (see Figure 1B, arrowheads). Similar results showing peripheral and contralateral annexin A5-positive cells have been published in a transient medial cerebral artery occlusion model.[22] An alternative hypothesis explaining annexin A5-positive regions without PI-uptake in our experiments would be a difference in vessels' permeability, selectively allowing the passage of large-molecular-weight proteins, such as annexin A5 protein, but not the smaller, yet charged, PI (BBB nonpenetrable),[36] perhaps because of modulation of transcellular and not paracellular vascular barriers.[42] However, the latter hypothesis, which may have led to underestimation of cell damage in our experiments utilizing PI, is

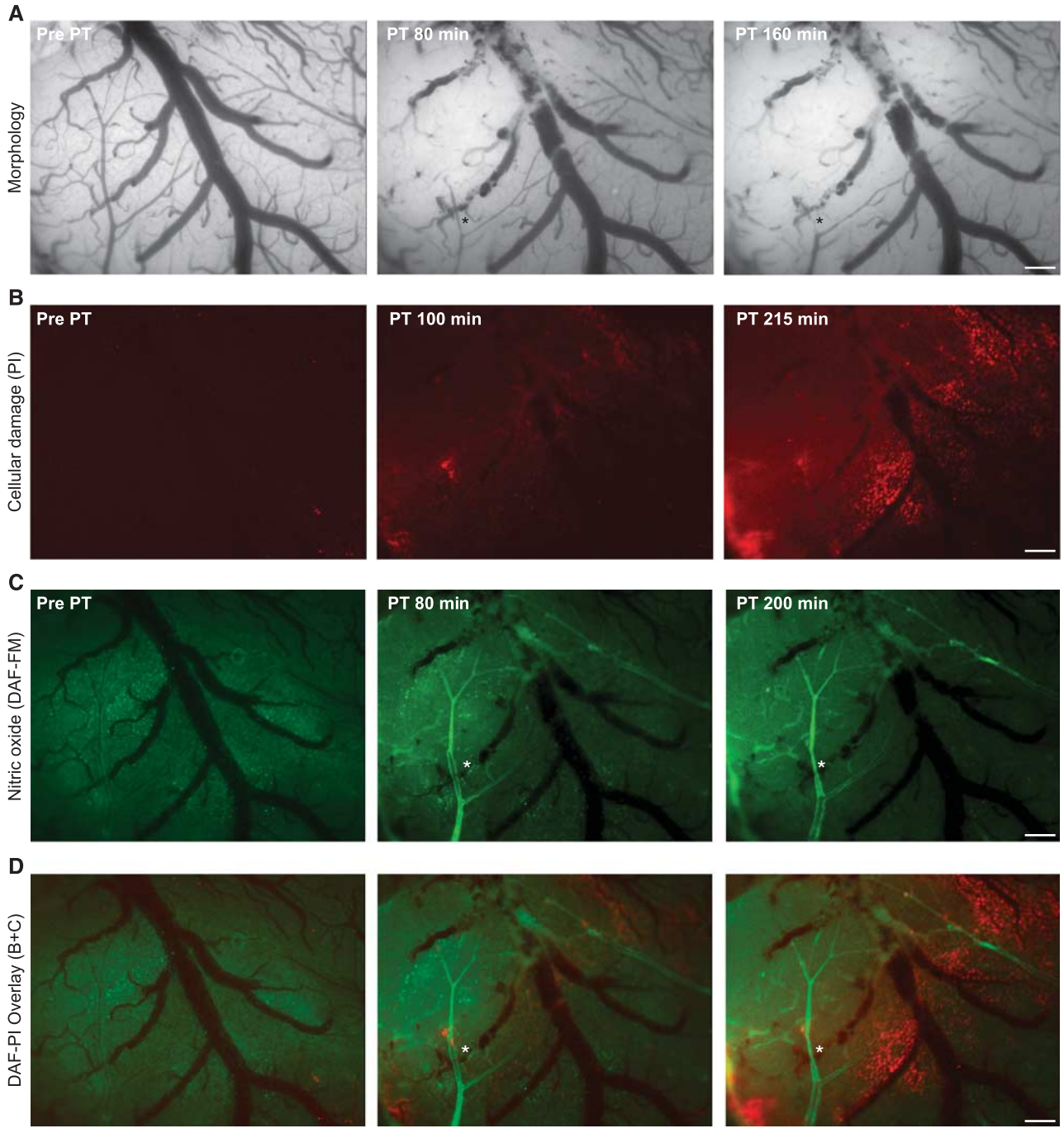

Figure 5. Intravital microscopy reveals nitric oxide (NO) formation after photothrombosis (PT). (**A**) From left to right: bright field images under control condition and 80 and 160 minutes after induction of PT. Note the lesion core in the top left corner. (**B**) Cell damage as visualized by propidium iodide (PI). (**C**) Nitric oxide as detected by 4-amino-5-methylamino-2′,7′-difluorofluorescein (DAF-FM) diacetate gave a diffuse parenchymal signal before PT and clearly showed arteriolar NO production at 80 and 200 minutes after PT in the ischemic core (here veins also revealed signal) and in the peri-ischemic arterioles. (**D**) Overlay of PI and DAF-FM. Note how cell damage is mainly concentrated surrounding venules. (**A**, **C,** and **D**) asterisk indicates arteriole that was primarily perfused after PT, however, underwent delayed constriction despite NO production. Scale bar = 200 μm.

less likely, since the region displaying BBB dysfunction (leakage of the charged tracer sodium fluorescein) clearly exceeded the region affected by cell damage, especially in animals treated with ROS inhibitors (Figures 3 and 6).

Our observation of progressive cell damage in the distant, apparently normally perfused, brain tissue is consistent with the notion that perfusion-based imaging methods may not detect regions eventually showing mild cell damage, and with the concept of selective neuronal loss in remote peri-ischemic regions.[43] Interestingly, we show here that normally perfused, remote peri-ischemic regions, are characterized by BBB dysfunction together with cellular damage. Accumulating results thus highlight imaging methods for the detection of a compromised BBB, as potentially sensitive for the detection of perilesional tissue at risk. In the nonischemic brain, experimental induction of BBB opening has been shown to induce neuronal damage preceded

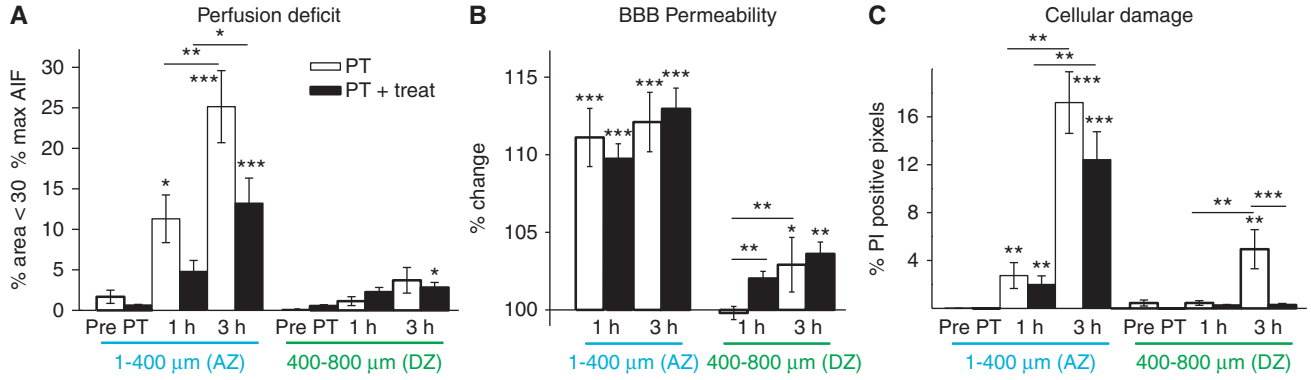

Figure 6. Quantification of perfusion deficit, blood–brain barrier (BBB) permeability, and cell damage after photothrombosis—involvement of free radical signaling. (**A**) Perfusion deficit was assessed as percentage of area not crossing 30% of the maximum of the arterial input function (maxAIF). Although under control conditions $< 1\%$ of the area was subthreshold ('hypoperfused', combined groups PT ($n = 7$) and PT+treat ($n = 9$)), the hypoperfused area increased in both the treated and nontreated group. Treatment reduced the hypoperfused area, however, not reaching significance. The distant peri-ischemic zone (400 to 800 μm from ischemic core) remained largely unaffected. (**B**) Blood–brain barrier permeability increased early and robustly in the adjacent peri-ischemic zone with progression to the distant peri-ischemic zone 3 hours after photothrombosis. Blood–brain barrier alterations remained unaffected by treatment. (**C**) Mild increases in cell damage were observed early in the adjacent peri-ischemic zone becoming more profound and progressing to the distant peri-ischemic zone after 3 hours. Cell damage in the distant peri-ischemic zone was reduced by inhibition of free radical signaling. Statistical analysis was performed with nonparametric paired Friedman's analysis of variance for related samples and Mann–Whitney *U*-test for independent samples including Bonferroni *post hoc* correction. Each ring of 100 μm width was represented by one mean value. $^{***}P < 0.001$; $^{**}P < 0.01$; $^{*}P < 0.05$. AZ, adjacent zone; DZ, distant peri-ischemic zone; PT, photothrombosis.

by the activation of astrocytes through serum-derived albumin and activation of inflammatory cascades.[6,9,11,44] Similar pathologic findings (e.g., glial activation) have been described in studies on selective neuronal loss and in the peri-ischemic brain after PT.[29,43] Future studies are awaited to confirm the role of BBB damage in nonischemic cellular damage and offer therapeutic strategies to facilitate its repair.

Several mechanisms have been described to underlie hypoperfusion, BBB dysfunction, and cell damage, among them energy depletion, excessive glutamate release, ionic imbalance (e.g., calcium overload, increased extracellular potassium), ROS production, peri-infarct depolarization and inflammatory response (e.g., via cytotoxic cytokines). Although morphologic correlates of the cellular immune response such as activated microglia, astrocytes, and blood-borne macrophages are only present ~1 day after the stroke, earlier deleterious events have been suggested to converge to free radical formation including excessive glutamate release, calcium overload, energy depletion, protease activation, NO synthetase uncoupling, and mitochondrial depolarization.[24,25,45] Conversely, NO may be essential to maintain or increase collateral blood flow in the peri-ischemic brain (see below) and reactive oxygen and nitrogen species were shown to be relevant cellular signaling molecules, involved in modulation of protein function and in angiogenesis.[46,47] Hence, prolonged interference with free radical signaling could be deleterious as it affects physiologic functions—a point that was raised to explain why clinical trials using free radical scavengers after stroke have largely failed.[47]

In vivo detection of free radical formation remains technically challenging. Despite the recent development of new small molecule indicators, most data still originate from *in vitro* models.[48] Recently, DAF-FM was successfully used to detect NO formation in the arterial and venous cerebral circulation after transient medial cerebral artery occlusion in the mice brain *in vivo*,[18] yet it is still to be uncovered which cells produce NO.[24] We report increased NO levels in the peri-ischemic brain, mostly in close vicinity to the arterial wall, suggesting a major nonneuronal contribution to NO formation. The source of superoxide and hydroxyl radicals remains elusive as we detected both vascular and parenchymal signal. Nitric oxide and superoxide together form toxic peroxynitrite that mediates pericyte constriction,[25] which in turn may lead to progressive cellular injury. The fact that we inhibited both superoxide/hydroxyl and NO formation, hence inhibited the NO scavenging effect of superoxide (which would result in peroxynitrite formation), may explain the lack of vasoconstriction despite NO scavenging. Although in the Yemisci *et al*[25] study inhibition of free radicals was associated with reversed constriction, we found a moderate (yet insignificant) reduction in hypoperfusion after free radical inhibition—perhaps because of topical (not intravenous) application in our study, the limited monitoring period (3 hours after PT in contrast to *ex vivo* analysis 6 hours after ischemia by Yemisci *et al*) or the small sample size. Our data are also consistent with the report by Kuntz *et al*[6] showing that BBB leakage coincides with emerging cell death. However, it is important to note that reducing cellular injury via free radical inhibition did not affect the extent of BBB breakdown, suggesting that BBB dysfunction in the distant peri-ischemic zone is not due to cell damage. The limited effect of ROS inhibition on perfusion is in line with recent studies in the slice preparation showing ischemia-induced pericyte-constriction associated with pericytic death shortly thereafter, and no significant involvement of ROS.[49] A surprising result was the lack of effect of ROS inhibition on the progression of BBB damage. Free radicals were previously shown to underlie ischemia-induced BBB dysfunction,[50] however, a major difference between the studies is the absence of reperfusion in the PT model we used. Reperfusion is known to result in a burst of additional ROS formation,[51] hence may aggravate ROS-induced neurovascular damage. Mechanisms underlying BBB breakdown may differ between models and brain regions exposed to permanent ischemia—and occlusion/reperfusion. Alternatively, since we started free radical inhibition 30 minutes after PT, there is still a theoretical possibility that free radical formation within that time window, initiated a cascade of events (even in the distant region) that lead to delayed BBB dysfunction.

In conclusion, the strength of our study lies in the parallel assessment of different physiologic parameters *in vivo*, allowing further in-depth studies into the mechanisms underlying brain damage in stroke models and testing of new therapeutics. The

nature of the PT lesion (reproducibility, clear ischemic core, and peri-ischemic tissue visible at the brain surface) is ideal for direct cortical imaging and its relevance for human cerebrovascular disease (including small vessel disease and vascular dementia) was recently highlighted.[52] We show new insights into the kinetics of hypoperfusion, BBB dysfunction, cell damage and free radical formation after vascular occlusion, and propose that clinical assessment of BBB permeability may help to delineate tissue at risk in patients.

DISCLOSURE/CONFLICT OF INTEREST

The authors declare no conflict of interest.

REFERENCES

1 Lozano R, Naghavi M, Foreman K, Lim S, Shibuya K, Aboyans V *et al.* Global and regional mortality from 235 causes of death for 20 age groups in 1990 and 2010: a systematic analysis for the Global Burden of Disease Study 2010. *Lancet* 2012; **380**: 2095–2128.
2 Ahmed N, Kellert L, Lees KR, Mikulik R, Tatlisumak T, Toni D. Results of intravenous thrombolysis within 4.5 to 6 hours and updated results within 3 to 4.5 hours of onset of acute ischemic stroke recorded in the Safe Implementation of Treatment in Stroke International Stroke Thrombolysis Register (SITS-ISTR): an observational study. *JAMA Neurol* 2013; **70**: 837–844.
3 Jauch EC, Saver JL, Adams HP, Bruno A, Connors JJB, Demaerschalk BM *et al.* Guidelines for the early management of patients with acute ischemic stroke: a guideline for healthcare professionals from the American Heart Association/ American Stroke Association. *Stroke* 2013; **44**: 870–947.
4 Astrup J, Symon L, Branston NM, Lassen NA. Cortical evoked potential and extracellular K+ and H+ at critical levels of brain ischemia. *Stroke* 1977; **8**: 51–57.
5 Latour LL, Kang D-W, Ezzeddine MA, Chalela JA, Warach S. Early blood-brain barrier disruption in human focal brain ischemia. *Ann Neurol* 2004; **56**: 468–477.
6 Kuntz M, Mysiorek C, Pétrault O, Pétrault M, Uzbekov R, Bordet R *et al.* Stroke-induced brain parenchymal injury drives blood-brain barrier early leakage kinetics: a combined in vivo/in vitro study. *J Cereb Blood Flow Metab* 2014; **34**: 95–107.
7 Dreier JP. The role of spreading depression, spreading depolarization and spreading ischemia in neurological disease. *Nat Med* 2011; **17**: 439–447.
8 Lapilover EG, Lippmann K, Salar S, Maslarova A, Dreier JP, Heinemann U *et al.* Peri-infarct blood-brain barrier dysfunction facilitates induction of spreading depolarization associated with epileptiform discharges. *Neurobiol Dis* 2012; **48**: 495–506.
9 Zlokovic B V. The blood-brain barrier in health and chronic neurodegenerative disorders. *Neuron* 2008; **57**: 178–201.
10 Balami JS, Chen R-L, Grunwald IQ, Buchan AM. Neurological complications of acute ischaemic stroke. *Lancet Neurol* 2011; **10**: 357–371.
11 Friedman A, Kaufer D, Heinemann U. Blood-brain barrier breakdown-inducing astrocytic transformation: novel targets for the prevention of epilepsy. *Epilepsy Res* 2009; **85**: 142–149.
12 Desilles J-P, Rouchaud A, Labreuche J, Meseguer E, Laissy J-P, Serfaty J-M *et al.* Blood-brain barrier disruption is associated with increased mortality after endovascular therapy. *Neurology* 2013; **80**: 844–851.
13 Hom J, Dankbaar JW, Soares BP, Schneider T, Cheng S-C, Bredno J *et al.* Blood-brain barrier permeability assessed by perfusion CT predicts symptomatic hemorrhagic transformation and malignant edema in acute ischemic stroke. *AJNR Am J Neuroradiol* 2011; **32**: 41–48.
14 Novotny HR, Alvis DL. A method of photographing fluorescence in circulating blood in the human retina. *Circulation* 1961; **24**: 82–86.
15 Van Vliet EA, Otte WM, Gorter JA, Dijkhuizen RM, Wadman WJ. Longitudinal assessment of blood-brain barrier leakage during epileptogenesis in rats. A quantitative MRI study. *Neurobiol Dis* 2014; **63**: 74–84.
16 Prager O, Chassidim Y, Klein C, Levi H, Shelef I, Friedman A. Dynamic in vivo imaging of cerebral blood flow and blood-brain barrier permeability. *Neuroimage* 2010; **49**: 337–344.
17 Serlin Y, Tal G, Chassidim Y, Parmet Y, Tomkins O, Knyazer B *et al.* Novel fluorescein angiography-based computer-aided algorithm for assessment of retinal vessel permeability. *PLoS One* 2013; **8**: e61599
18 Terpolilli NA, Kim S-W, Thal SC, Kataoka H, Zeisig V, Nitzsche B *et al.* Inhalation of nitric oxide prevents ischemic brain damage in experimental stroke by selective dilatation of collateral arterioles. *Circ Res* 2012; **110**: 727–738.
19 Kundu K, Knight SF, Willett N, Lee S, Taylor WR, Murthy N. Hydrocyanines: a class of fluorescent sensors that can image reactive oxygen species in cell culture, tissue, and in vivo. *Angew Chem Int Ed Engl* 2009; **48**: 299–303.
20 Selvam S, Kundu K, Templeman KL, Murthy N, García AJ. Minimally invasive, longitudinal monitoring of biomaterial-associated inflammation by fluorescence imaging. *Biomaterials* 2011; **32**: 7785–7792.
21 Bahmani P, Schellenberger E, Klohs J, Steinbrink J, Cordell R, Zille M *et al.* Visualization of cell death in mice with focal cerebral ischemia using fluorescent annexin A5, propidium iodide, and TUNEL staining. *J Cereb Blood Flow Metab* 2011; **31**: 1311–1320.
22 Blankenberg FG, Kalinyak J, Liu L, Koike M, Cheng D, Goris ML *et al.* 99mTc-HYNIC-annexin V SPECT imaging of acute stroke and its response to neuroprotective therapy with anti-Fas ligand antibody. *Eur J Nucl Med Mol Imaging* 2006; **33**: 566–574.
23 Pacher P, Beckman JS, Liaudet L. Nitric oxide and peroxynitrite in health and disease. *Physiol Rev* 2007; **87**: 315–424.
24 Moskowitz M a, Lo EH, Iadecola C. The science of stroke: mechanisms in search of treatments. *Neuron* 2010; **67**: 181–198.
25 Yemisci M, Gursoy-Ozdemir Y, Vural A, Can A, Topalkara K, Dalkara T. Pericyte contraction induced by oxidative-nitrative stress impairs capillary reflow despite successful opening of an occluded cerebral artery. *Nat Med* 2009; **15**: 1031–1037.
26 Watson BD, Dietrich WD, Busto R, Wachtel MS, Ginsberg MD. Induction of reproducible brain infarction by photochemically initiated thrombosis. *Ann Neurol* 1985; **17**: 497–504.
27 Schellenberger EA, Weissleder R, Josephson L. Optimal modification of annexin V with fluorescent dyes. *Chembiochem* 2004; **5**: 271–274.
28 Stoll G, Kleinschnitz C, Meuth SG, Braeuninger S, Ip CW, Wessig C *et al.* Transient widespread blood–brain barrier alterations after cerebral photothrombosis as revealed by gadofluorine M-enhanced magnetic resonance imaging. *J Cereb Blood Flow Metab* 2009; **29**: 331–341.
29 Levi H, Schoknecht K, Prager O, Chassidim Y, Weissberg I, Serlin Y *et al.* Stimulation of the sphenopalatine ganglion induces reperfusion and blood-brain barrier protection in the photothrombotic stroke model. *PLoS One* 2012; **7**: e39636.
30 Wang HK, Miyachi S, Yamazaki M, Sawada Y, Chung YB, Iga T *et al.* Nonlinear pharmacokinetics of hepatobiliary transport of rose bengal in rats after iv bolus administration with varying doses. *Biopharm Drug Dispos* 1992; **13**: 647–662.
31 Arndt-Jovin DJ, Jovin TM. Fluorescence Microscopy of Living Cells in Culture Part B. Quantitative Fluorescence Microscopy—Imaging and Spectroscopy. *Methods in Cell Biol* 1989; **30**: 1–503. ii-xiv.
32 Hossmann KA. Viability thresholds and the penumbra of focal ischemia. *Ann Neurol* 1994; **36**: 557–565.
33 Dani KA, Thomas RGR, Chappell FM, Shuler K, MacLeod MJ, Muir KW *et al.* Computed tomography and magnetic resonance perfusion imaging in ischemic stroke: definitions and thresholds. *Ann Neurol* 2011; **70**: 384–401.
34 Chassidim Y, Veksler R, Lublinsky S, Pell GS, Friedman A, Shelef I. Quantitative imaging assessment of blood-brain barrier permeability in humans. *Fluids Barriers CNS* 2013; **10**: 9.
35 Kaufmann AM, Firlik AD, Fukui MB, Wechsler LR, Jungries CA, Yonas H. Ischemic core and penumbra in human stroke. *Stroke* 1999 **30**: 93–99.
36 Unal Cevik I, Dalkara T. Intravenously administered propidium iodide labels necrotic cells in the intact mouse brain after injury. *Cell Death Differ* 2003; **10**: 928–929.
37 Blankenberg FG. In vivo detection of apoptosis. *J Nucl Med* 2008; **49 Suppl 2**: 81S–95S.
38 Braun JS, Jander S, Schroeter M, Witte OW, Stoll G. Spatiotemporal relationship of apoptotic cell death to lymphomonocytic infiltration in photochemically induced focal ischemia of the rat cerebral cortex. *Acta Neuropathol* 1996; **92**: 255–263.
39 Van Hoecke M, Prigent-Tessier A, Bertrand N, Prevotat L, Marie C, Beley A. Apoptotic cell death progression after photothrombotic focal cerebral ischaemia: effects of the lipophilic iron chelator 2,2′-dipyridyl. *Eur J Neurosci* 2005; **22**: 1045–1056.
40 Schroeter M, Jander S, Huitinga I, Witte OW, Stoll G. Phagocytic response in photochemically induced infarction of rat cerebral cortex. The role of resident microglia.*Stroke* 1997; **28**: 382–386.
41 Li H, Zhang N, Lin H, Yu Y, Cai Q-Y, Ma L *et al.* Histological, cellular and behavioral assessments of stroke outcomes after photothrombosis-induced ischemia in adult mice. *BMC Neurosci* 2014; **15**: 58.
42 Kang EJ, Major S, Jorks D, Reiffurth C, Offenhauser N, Friedman A *et al.* Blood-brain barrier opening to large molecules does not imply blood-brain barrier opening to small ions. *Neurobiol Dis* 2013; **52**: 204–218.
43 Baron J-C, Yamauchi H, Fujioka M, Endres M. Selective neuronal loss in ischemic stroke and cerebrovascular disease. *J Cereb Blood Flow Metab* 2014; **34**: 2–18.
44 Bar-Klein G, Cacheaux LP, Kamintsky L, Prager O, Weissberg I, Schoknecht K *et al.* Losartan prevents acquired epilepsy via TGF-β signaling suppression. *Ann Neurol* 2014; **75**: 864–875.
45 Dirnagl U, Iadecola C, Moskowitz M a. Pathobiology of ischaemic stroke: an integrated view. *Trends Neurosci* 1999; **22**: 391–397.

46 Rhee SG. Cell signaling. H2O2, a necessary evil for cell signaling. *Science* 2006; **312**: 1882–1883.
47 Lo EH. A new penumbra: transitioning from injury into repair after stroke. *Nat Med* 2008; **14**: 497–500.
48 Wang X, Fang H, Huang Z, Shang W, Hou T, Cheng A *et al.* Imaging ROS signaling in cells and animals. *J Mol Med (Berl)* 2013; **91**: 917–927.
49 Hall CN, Reynell C, Gesslein B, Hamilton NB, Mishra A, Sutherland BA *et al.* Capillary pericytes regulate cerebral blood flow in health and disease. *Nature* 2014; **508**: 55–60.
50 Pun PBL, Lu JIA, Moochhala S. Involvement of ROS in BBB dysfunction. *Environ Res* 2009; **43**: 348–364.
51 Peters O, Back T, Lindauer U, Busch C, Megow D, Dreier J *et al.* Increased formation of reactive oxygen species after permanent and reversible middle cerebral artery occlusion in the rat. *J Cereb Blood Flow Metab* 1998; **18**: 196–205.
52 Shih AY, Blinder P, Tsai PS, Friedman B, Stanley G, Lyden PD *et al.* The smallest stroke: occlusion of one penetrating vessel leads to infarction and a cognitive deficit. *Nat Neurosci* 2013; **16**: 55–63.

Supplementary Information accompanies the paper on the Journal of Cerebral Blood Flow & Metabolism website (http://www.nature.com/jcbfm)

Mein Lebenslauf wird aus datenschutzrechtlichen Gründen in der elektronischen Version meiner Arbeit nicht veröffentlicht.

Publications

1) Original Contributions

Schoknecht K, Prager O, Vazana U, Kamintsky L, Harhausen D, Zille M, Figge L, Chassidim Y, Schellenberger E, Kovács R, Heinemann U, Friedman A. Monitoring stroke progression: in vivo imaging of cortical perfusion, blood-brain barrier permeability and cellular damage in the rat photothrombosis model. J Cereb Blood Flow Metab 2014:34/11,1791-80.

Bar-Klein G, Cacheaux LP, Kamintsky L, Prager O, Weissberg I, **Schoknecht K**, Cheng P, Kim SY, Wood L, Heinemann U, Kaufer D, Friedman A. Losartan prevents acquired epilepsy via TGF-β signaling suppression. Ann Neurol 2014:75/6,864-75.

Levi H, **Schoknecht K**, Prager O, Chassidim Y, Weissberg I, Serlin Y, Friedman A. Stimulation of the sphenopalatine ganglion induces reperfusion and blood-brain barrier protection in the photothrombotic stroke model. PLoS One 2012:7/6,e39636.

Ofek K, **Schoknecht K**, Melamed-Book N, Heinemann U, Friedman A, Soreq H. Fluoxetine induces vasodilatation of cerebral arterioles by co-modulating NO/muscarinic signalling. J Cell Mol Med 2012:16/11,2736-44.

2) Reviews

Heinemann U, Milikovsky D, Veksler R, **Schoknecht K.** Inflammation und Blut-Hirn-Schranke. Zeitschrift für Epileptol 2015 (DOI: 10.1007/s10309-015-0010-9).

Schoknecht K, David Y, Heinemann U. The blood–brain barrier—Gatekeeper to neuronal homeostasis: Clinical implications in the setting of stroke. Semin Cell Dev Biol 2015:38/35-42.

Chassidim Y, Vazana U, Prager O, Veksler R, Bar-Klein G, **Schoknecht K**, Fassler M, Lublinsky S, Shelef I. Analyzing the blood-brain barrier: The benefits of medical imaging in research and clinical practice. Semin Cell Dev Biol 2015:38/43-52.

Schoknecht K, Shalev H. Blood-brain barrier dysfunction in brain diseases: clinical experience. Epilepsia 2012:53/6,7-13.

Wunder A, **Schoknecht K**, Stanimirovic DB, Prager O, Chassidim Y. Imaging blood-brain barrier dysfunction in animal disease models. Epilepsia 2012:53/6,14-21.

3) Case reports

Schoknecht K, Gabi S, Ifergane G, Friedman A, Shelef I. Detection of Cerebral Hyperperfusion Syndrome after Carotid Endarterectomy with CT Perfusion. J Neuroimaging 2014:24/3,295-7.

Acknowledgements

Throughout my PhD I was very lucky with the people around me – both in Germany and in Israel. It always felt warm and I hope I managed to show a good share of my gratitude ‘online’, long before writing this page. Being able to travel the world, especially all these months in Israel, added unforgettable experiences to my PhD (here we are leaving the work on the bench). This was only possible because:

1) Uwe Heinemann gave me all this freedom to make my PhD a bi-national project,

2) Alon Friedman was such a hospitable person and created such a friendly environment in his laboratory and in Sde Boker, and

3) my longest non-scientific supervisors (expanding numerous generations) never stopped supporting me, even when I wasn’t in the most calming place.

I once more have to highlight the people that appear on the publication and in addition want to thank Andreas Wunder and Jens Dreier for their advice.

Thank you all very much!